Supplementary Information for:

Photoresponsive ionic Hydrogen-Bonded Organic Framework exhibiting pyridine protonation effects achieve room-temperature phosphorescence through polymer doping

Jia-Yu Wang, Bin Zhou and Li-Hui Cao*

[a]Shaanxi Key Laboratory of Chemical Additives for Industry, College of Chemistry and Chemical Engineering, Shaanxi University of Science and Technology, Xi'an, 710021, P. R. China

E-mail: caolihui@sust.edu.cn

Materials methods and experimental details

Materials and reagents.

All reagents and solvents, including 1,3,5-triphenylbenzene, tris(4-pyridyl) amine (TPA), polyvinyl alcohol (PVA), 1,4-dioxane, concentrated sulfuric acid and ethyl acetate were obtained from commercial suppliers and used as received. Deionized water was used throughout the experimental procedures.

Preparation of ligand (H_3SPB).

Based on the literature method, the sulfonic acid-substituted 1,3,5-triphenylbenzene ligand (H_3SPB) was synthesized using an improved protocol. Concentrated sulfuric acid (ca. 98%, 15 mL) was added to 1,3,5-triphenylbenzene (5 g), and the mixture was heated at 110 °C for 16 h under a nitrogen atmosphere. The hot mixture was then poured into deionized water (100 mL). The product was washed with an excess of ethyl acetate, followed by filtration and drying.[1]

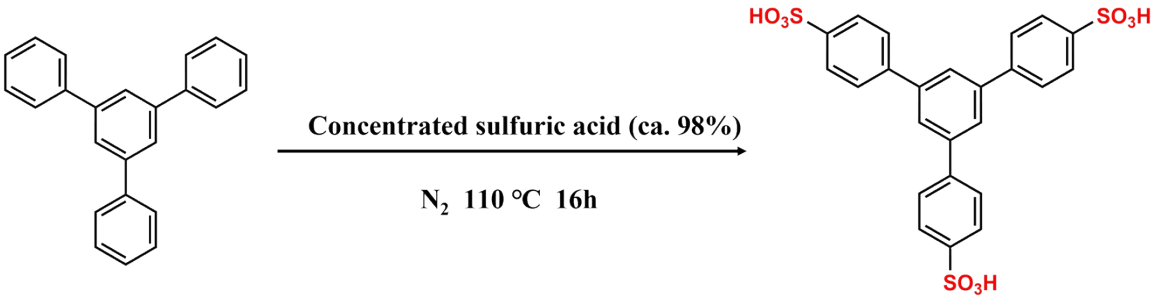

Scheme S1. Schematic representation for preparation of compound H_3SPB.

Preparation of iHOF-71.

TPA (2.5 mg, 0.010 mmol) was dissolved in 2 mL of H_2O, followed by the addition of 15 μL of 1 mol/L HCl solution to achieve complete dissolution. Separately, H_3SPB (5.5 mg, 0.010 mmol) was dissolved in 2 mL of 1,4-dioxane to give a clear solution, to which 15 μL of 1 mol/L HCl solution was added under stirring to ensure homogeneous dispersion. The two solutions were then thoroughly combined and allowed to stand at room temperature. The vessel was covered with plastic film pierced with small holes for slow solvent evaporation. Colorless transparent rod-shaped crystals were obtained after 1 day.

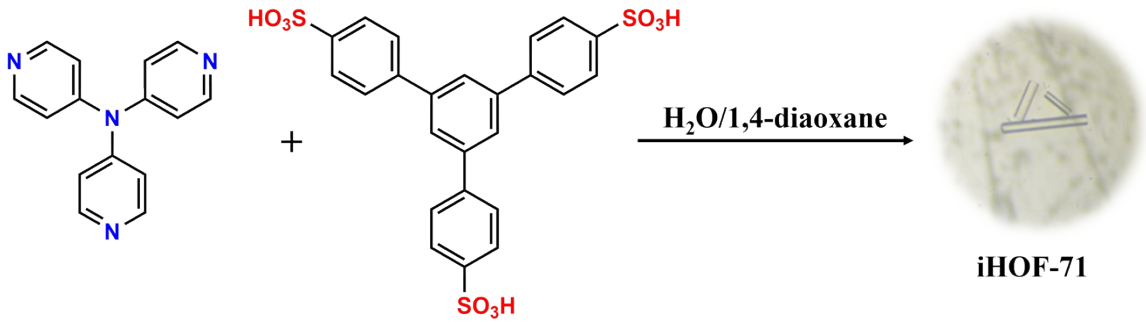

Scheme S2. Schematic representation for preparation of compound **iHOF-71**. (The inset on the right shows a microscope image.)

Preparation of 5%- iHOF-71@PVA composite membrane.

10 wt % PVA (2 g) was added to 2 mL of water and stirred for 15 min to form a well-dispersed mixture. Separately, **iHOF-71** (10 mg) was thoroughly ground and then dispersed in 2 mL of water under stirring for 6 h

to obtain a uniform suspension. The two mixtures were combined and stirred continuously at room temperature for 6 h, resulting in a homogeneous solution. The resulting mixture was cast into a glass mold and dried in an oven at 70 °C for 5 h to remove the solvent, resulting in a **5%-iHOF-71@PVA** composite membrane.[2]

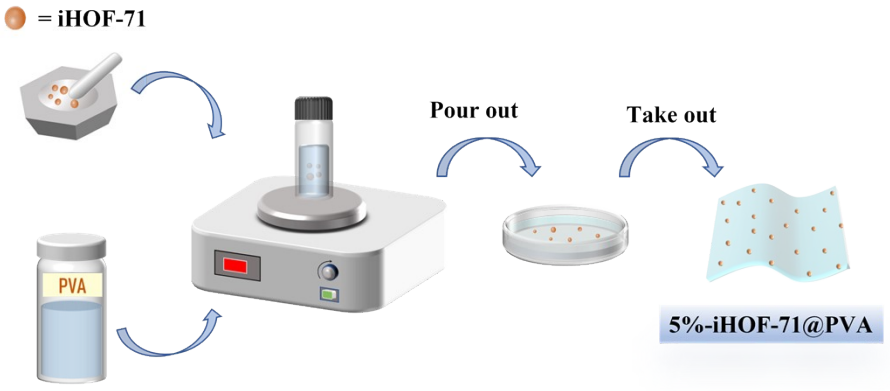

Figure S1. The **5%-iHOF-71@PVA** composite membrane production process.

Characterization.

The Powder X-ray diffraction (PXRD) measurements were carried out in Bruker D8 Advance with a Cu X-ray source over a range of 2θ = 5.0-50.0º. Fourier transform infrared (FT-IR) spectra were recorded on a Vector-22 spectrometer in the range of 4000-400 cm^{-1} using potassium bromide pellets. Solid-state UV-vis spectra were recorded on an Agilent Cary 5000 spectrophotometer. Optical properties were tested on a FLS1000 steady-state transient fluorescence spectrometer in Edinburgh. ^{1}H NMR spectra were

recorded on a Bruker 400 MHz spectrometer, with chemical shifts reported in ppm. Thermogravimetric analysis (TGA) was performed on TGA-55 under a nitrogen atmosphere at a heating rate of 10 °C/min over a temperature range of 30 to 600 °C. X-ray photoelectron spectroscopy (XPS) measurements were performed on a Thermo Fisher Nexsa spectrometer, with the binding energy scale calibrated using the C 1s peak at 284.8 eV as an internal reference. The solid-state EPR spectra were recorded at ambient temperature with a Bruker A300 Electron Spin Resonance Spectrometer.

Single-Crystal X-ray Diffraction.

Single-crystal X-ray diffraction data for compound **iHOF-71** was collected on a Bruker D8 Venture three-circle diffractometer equipped with a Bruker PHOTON-II area detector and graphite-monochromated Mo-Kα radiation (λ = 0.71073 Å) using φ-scan and ω-scan. Data processing was performed using the SAINT program, with Lorentz and polarization corrections applied. Absorption corrections were implemented via the SADABS program.[3] The structure was solved with direct methods (SHELXS) and refined by full-matrix least squares on F^2 using OLEX2, which utilizes the SHELXL-2019/3 module.[4,5] All non-hydrogen atoms were refined anisotropically. Displacement parameter restraints were used in modeling the ligands. Hydrogen atoms were placed geometrically on their riding atom where

possible. 93 water molecules are included in the unit cell as solvent. Crystal data containing space group, lattice parameters and other relevant information for the title complex are summarized in Table S1. More details on the crystallographic data are given in the X-ray crystallographic files in CIF format. Complete structural data have been deposited with the Cambridge Crystallographic Data Centre under reference number CCDC 2488490 for **iHOF-71**.

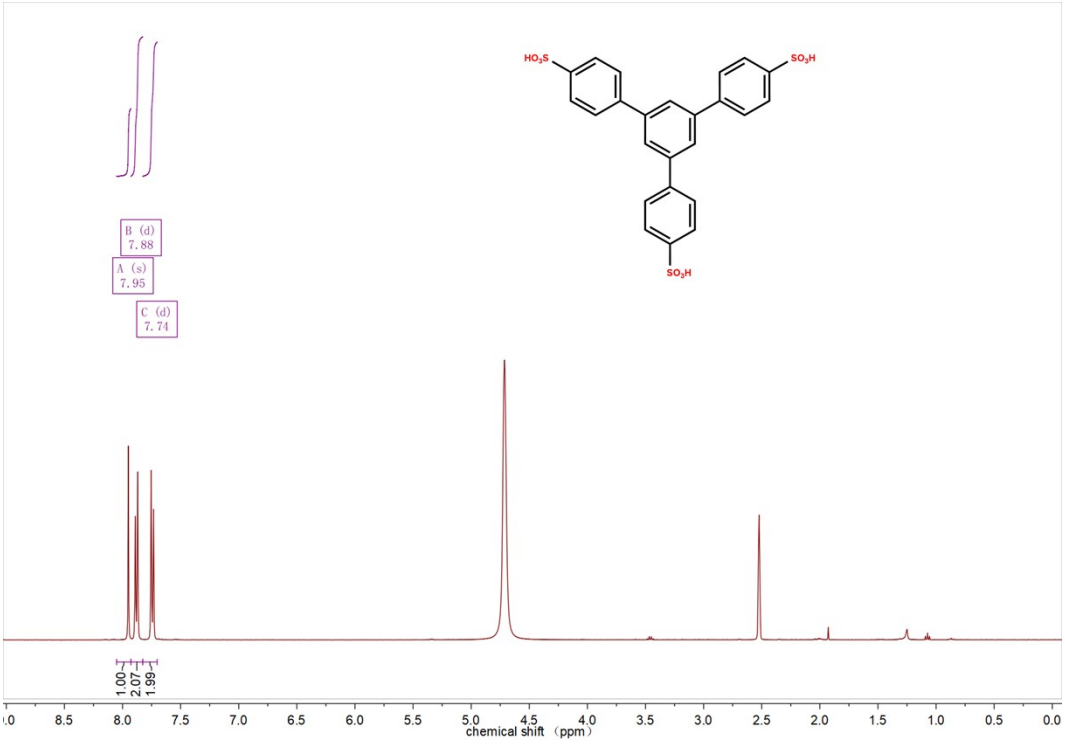

Figure S2. ^{1}H NMR synthesized by H_3SPB.

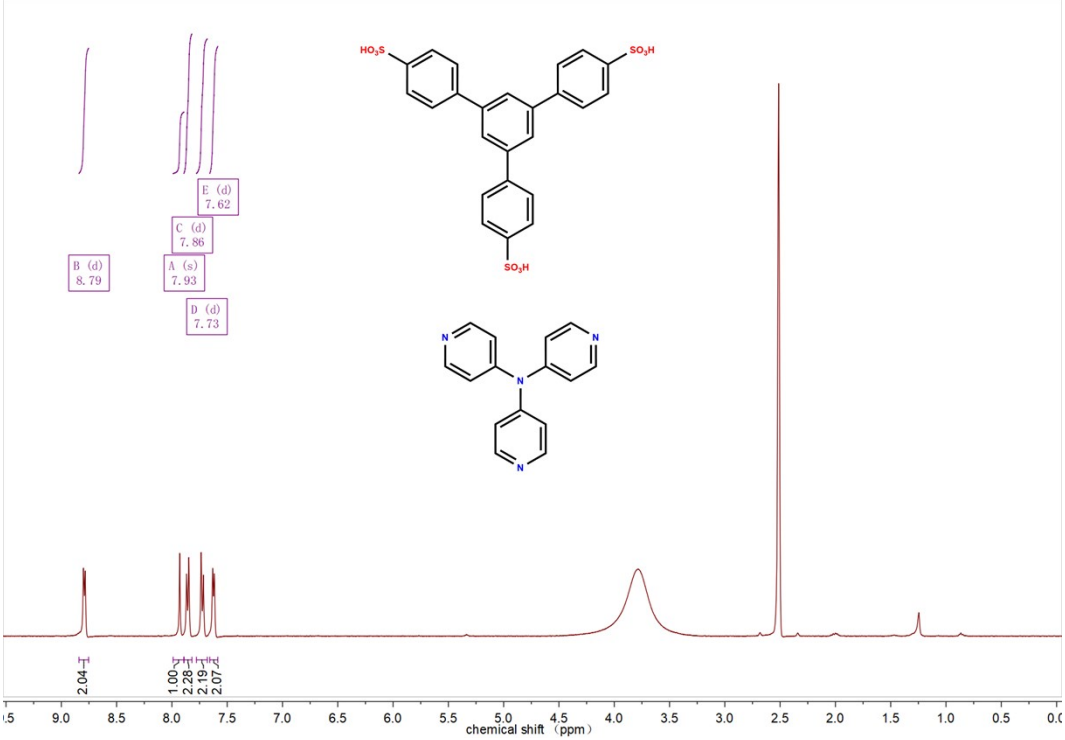

Figure S3. ^{1}H NMR spectrum of **iHOF-71**.

Computational Details

All density functional theory (DFT) calculations were performed using the CP2K 2025.2 software package within the Gaussian and plane waves (GPW) framework. The exchange-correlation interactions were described by the Perdew–Burke–Ernzerhof (PBE) functional, augmented with Grimme's D3 dispersion correction with Becke–Johnson damping. For geometry optimizations, the valence electrons were described by the DZVP-MOLOPT-SR-GTH basis set, while the core electrons were represented by the GTH-PBE pseudopotentials. The energy cutoff and the relative cutoff were set to 600 Ry and 55 Ry, respectively. The Brillouin zone integration was restricted to the Γ-point. Time-dependent DFT (TD-DFT) calculations were subsequently conducted employing the same functional, but the TZVP-MOLOPT-SR-GTH basis set alongside GTH-SOC-PBE pseudopotentials. The lowest 50 singlet and 50 triplet excited states were computed. Furthermore, the spin-orbit coupling (SOC) matrix elements among the lowest 20 excited states were evaluated.

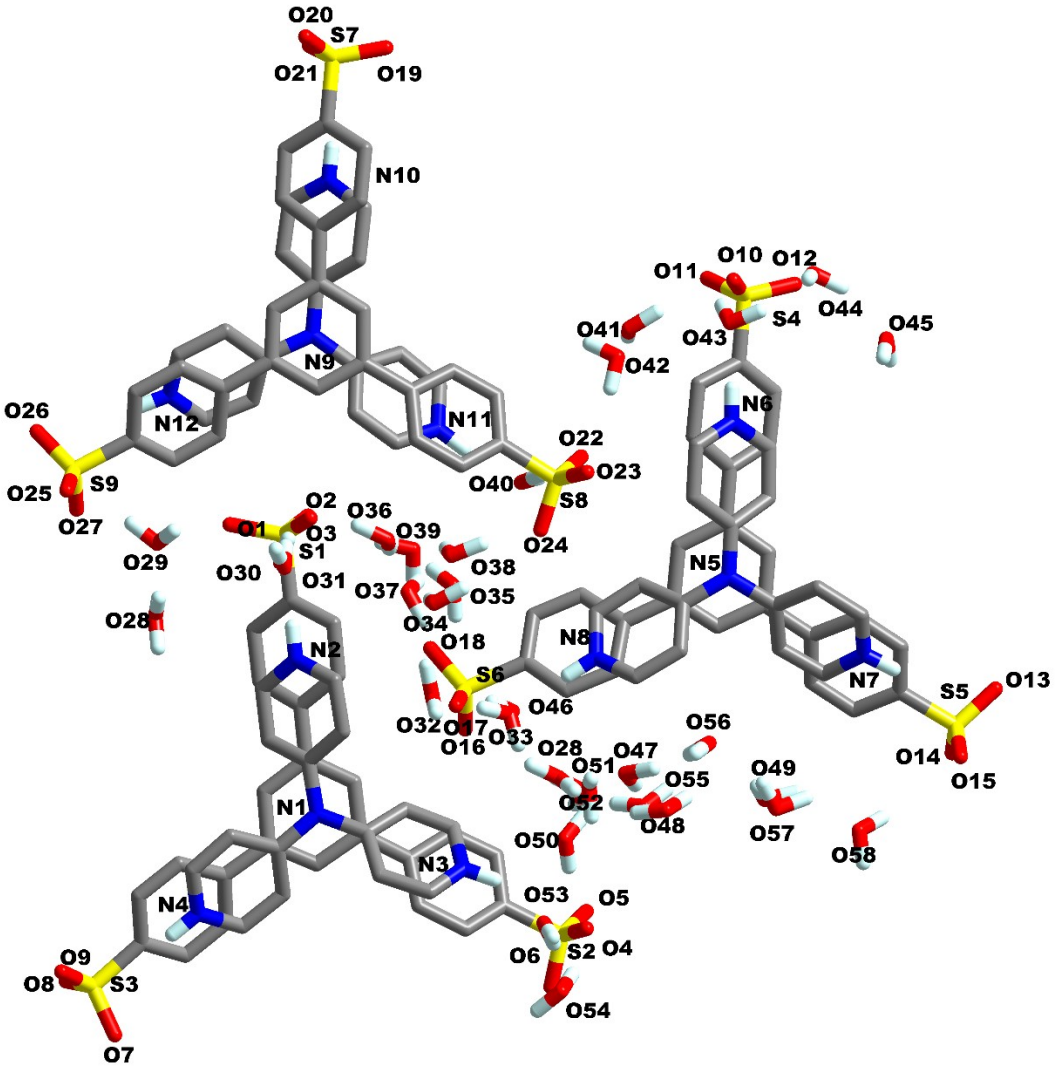

Figure S4. The asymmetric unit of **iHOF-71**. (The H atoms on the structural units have been omitted for clarity. The asymmetric unit contains 31 solvent water molecules. O (1-58): red; N (1-12): blue; S (1-9): yellow.)

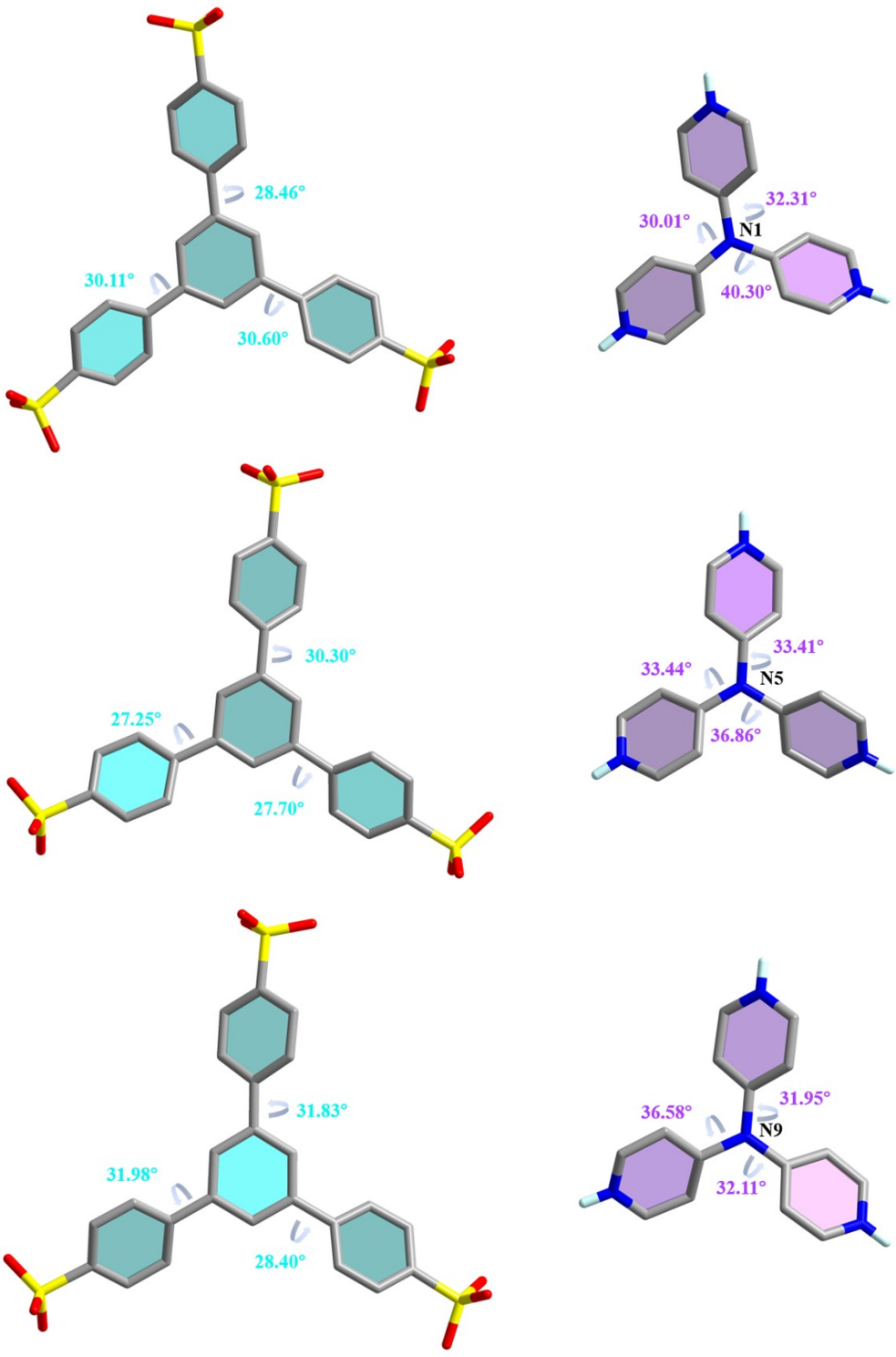

Figure S5. The torsion angles of the molecule in the asymmetric unit of **iHOF-71**.

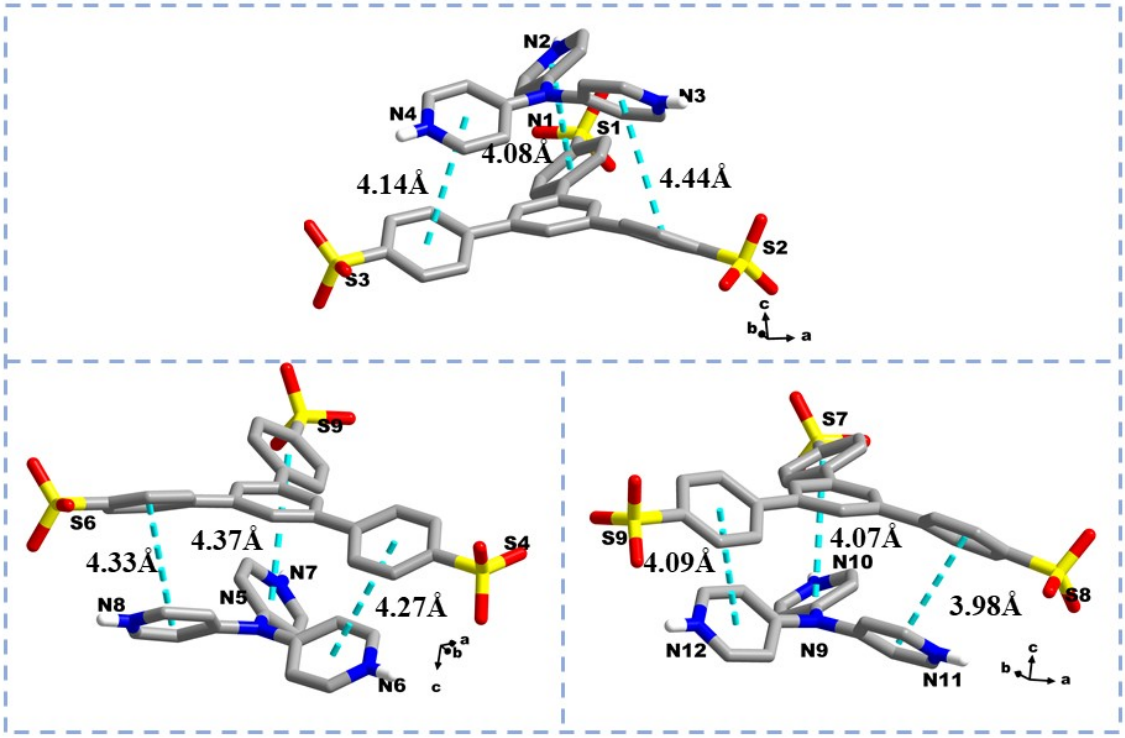

Figure S6. π-π stacking in **iHOF-71**.

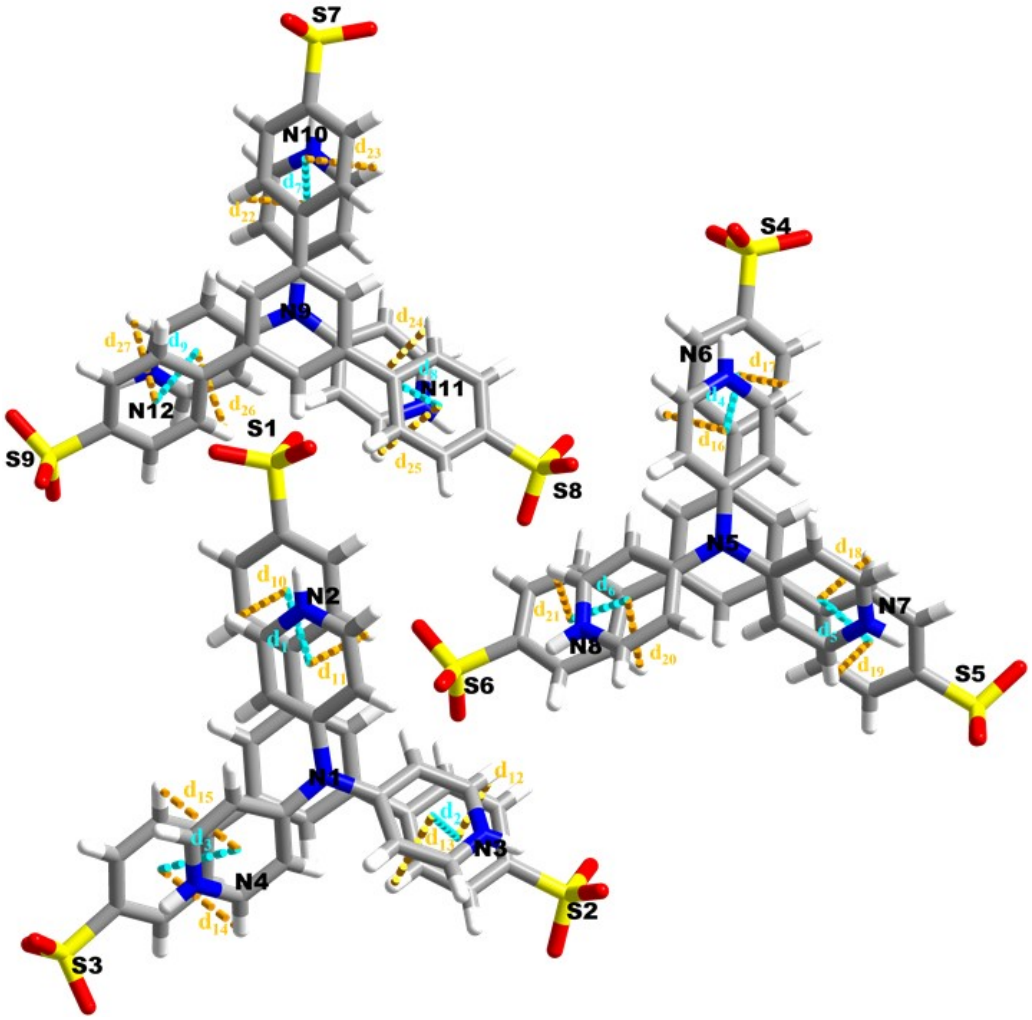

d_1=3.21Å d_{10}=3.22Å d_{16}=3.47Å d_{22}=3.09Å
d_2=4.44Å d_{11}=3.48Å d_{17}=3.33Å d_{23}=3.09Å
d_3=4.14Å d_{12}=3.56Å d_{18}=3.38Å d_{24}=3.09Å
d_4=4.27Å d_{13}=3.67Å d_{19}=3.15Å d_{25}=3.09Å
d_5=4.35Å d_{14}=3.44Å d_{20}=3.51Å d_{26}=3.09Å
d_6=4.32Å d_{15}=3.42Å d_{21}=3.09Å d_{27}=3.09Å
d_7=4.07Å
d_8=3.96Å
d_9=4.09Å

Figure S7. Schematic diagram of intermolecular interactions in **iHOF-71**.

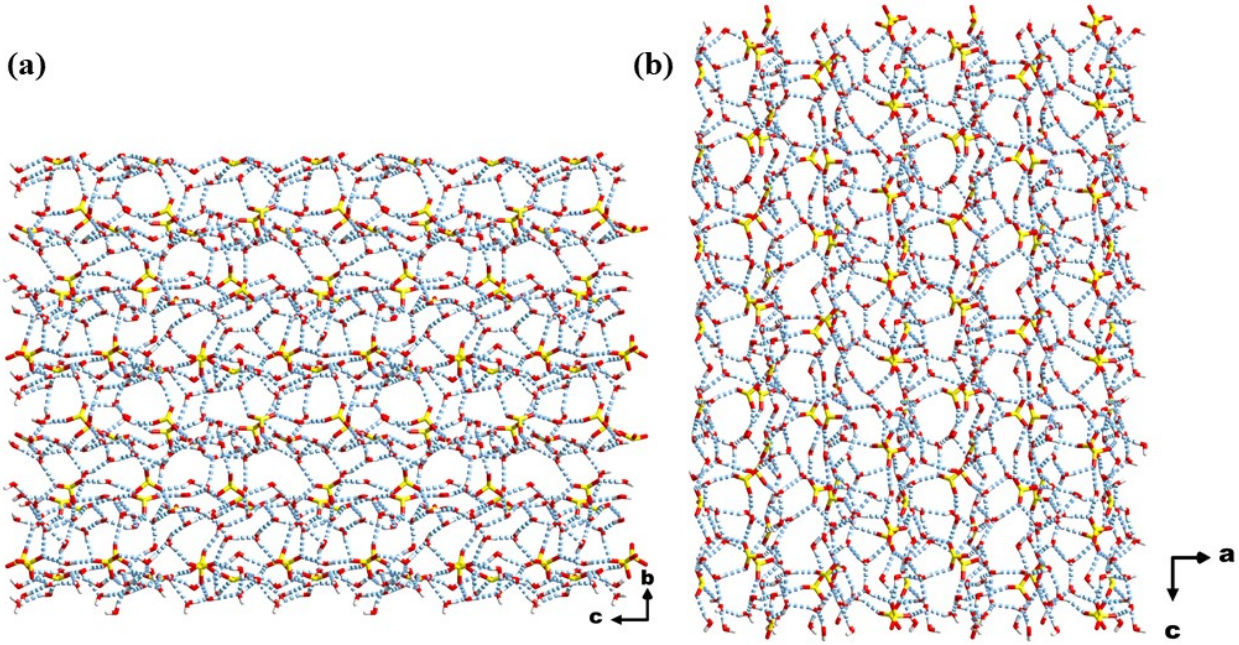

Figure S8. Hydrogen-bonded network structure of **iHOF-71** along the (a) *a*-axis and (b) *b*-axis directions.

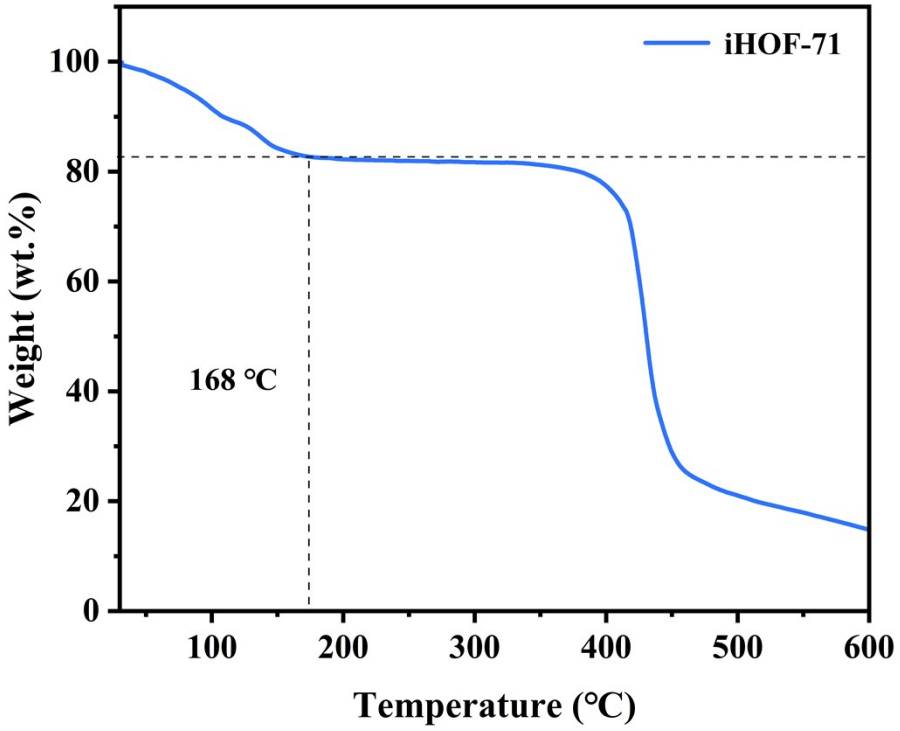

Figure S9. TGA plot of **iHOF-71**.

To evaluate the stability of **iHOF-71**, thermogravimetric analysis (TGA) was performed. The TGA curve reveals that the thermal decomposition of the material proceeds through two distinct weight-loss stages. The mass loss observed between room temperature and 168 °C corresponds to the loss of solvent water molecules. Following the plateau region between 168 °C and 360 °C, the collapse of the framework leads to destruction of the molecular structure, resulting in further mass loss.

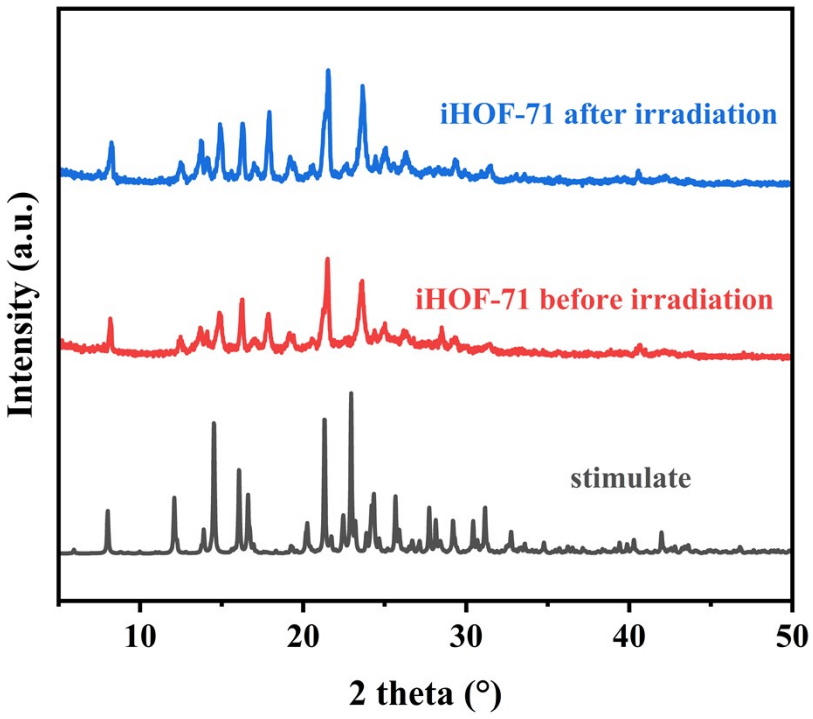

Figure S10. PXRD patterns of **iHOF-71**.

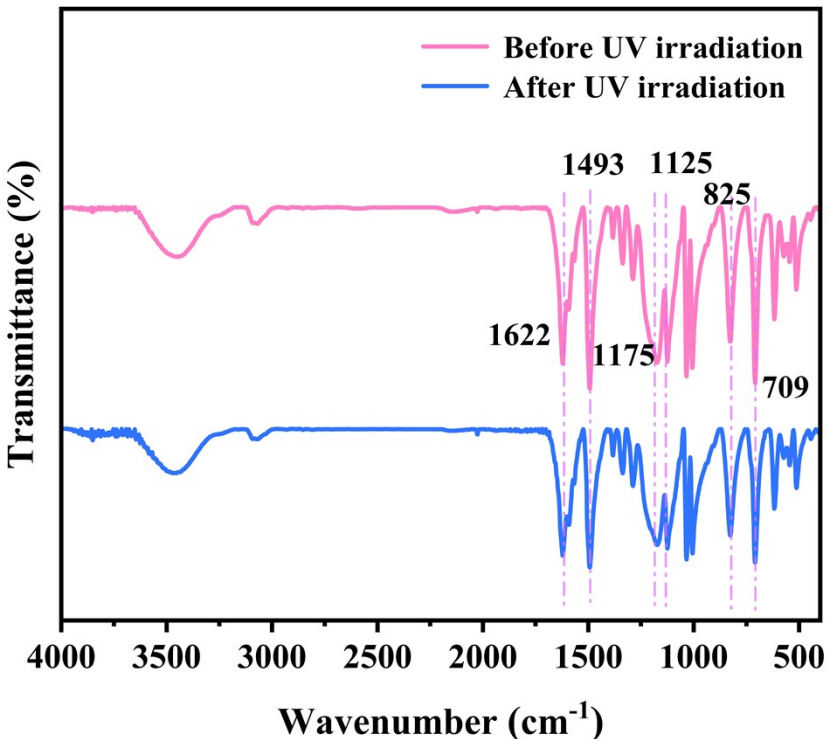

Figure S11. FT-IR spectra of **iHOF-71**.

The FT-IR spectra confirm the structural features of the framework: a broad band at 3650-3270 cm^{-1} corresponds to O–H stretching from crystalline water and hydrogen bond network, while the peak at 1622 cm^{-1} arises from H–O–H bending. The aromatic skeleton is indicated by a strong absorption at 1493 cm^{-1} (C=C/C=N^{+} stretching). Peaks at 1175 and 1125 cm^{-1} are attributed to asymmetric stretching of –SO^{3-} groups, and those at 825 cm^{-1} and 709 cm^{-1} correspond to out-of-plane C–H bending of 1,3,5-trisubstituted and monosubstituted benzene rings, respectively. Together, these spectroscopic features confirm the formation of a rigid three-dimensional iHOF.

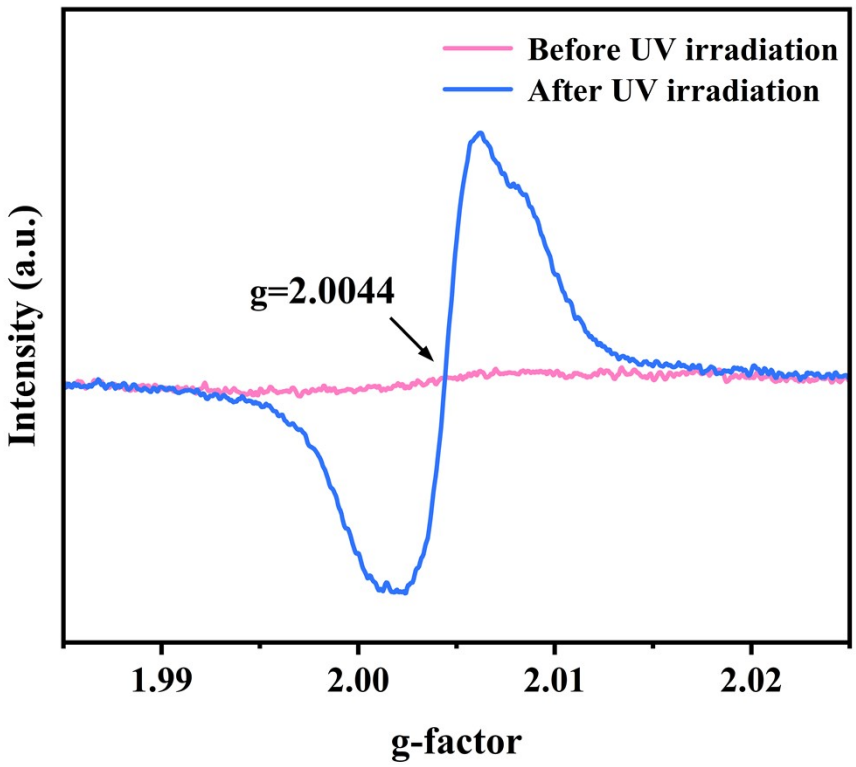

Figure S12. EPR spectra of **iHOF-71**.

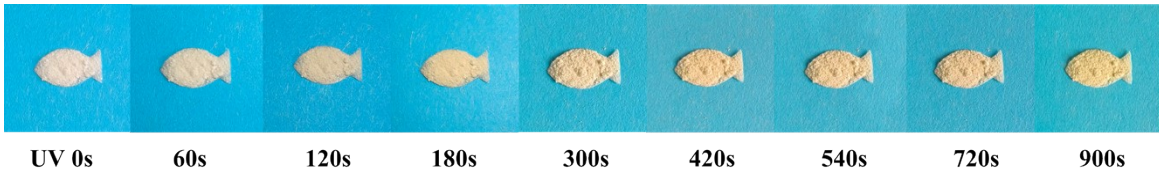

Figure S13. Photochromic photographs of **iHOF-71** powder.

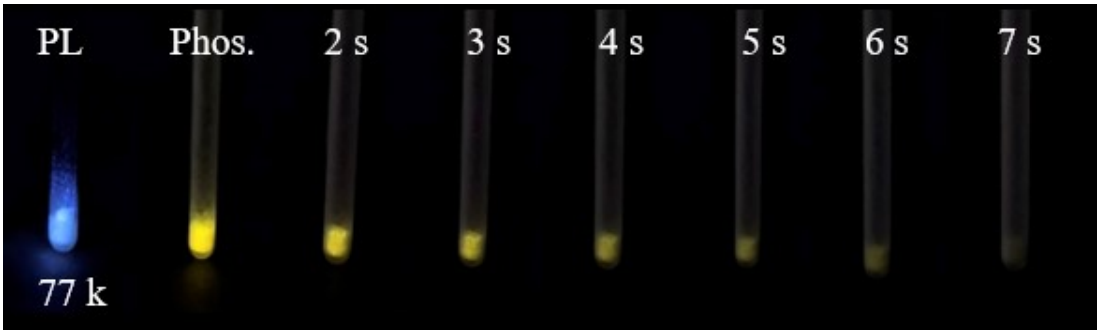

Figure S14. Photographs showing the time-dependent decay of fluorescence and afterglow for **iHOF-71** at 77 K.

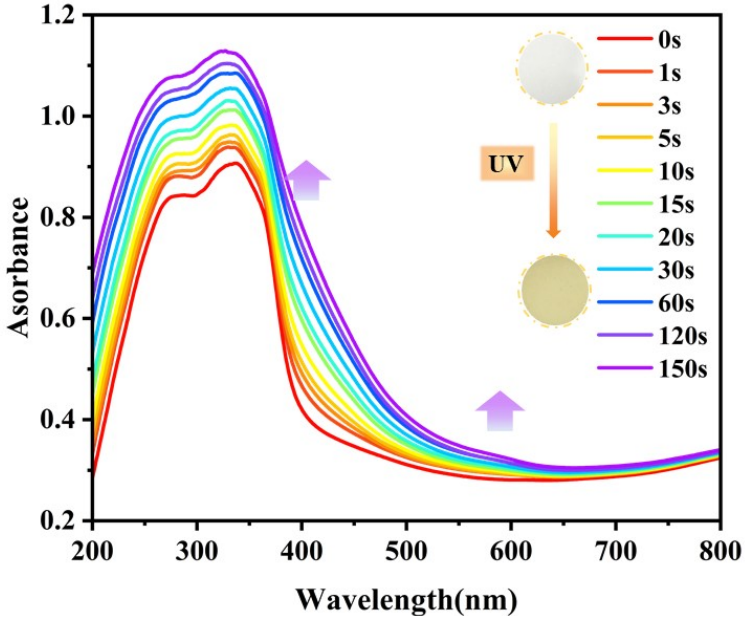

Figure S15. Solid UV-vis absorption spectra of **iHOF-71** before and after 365 nm UV irradiation.

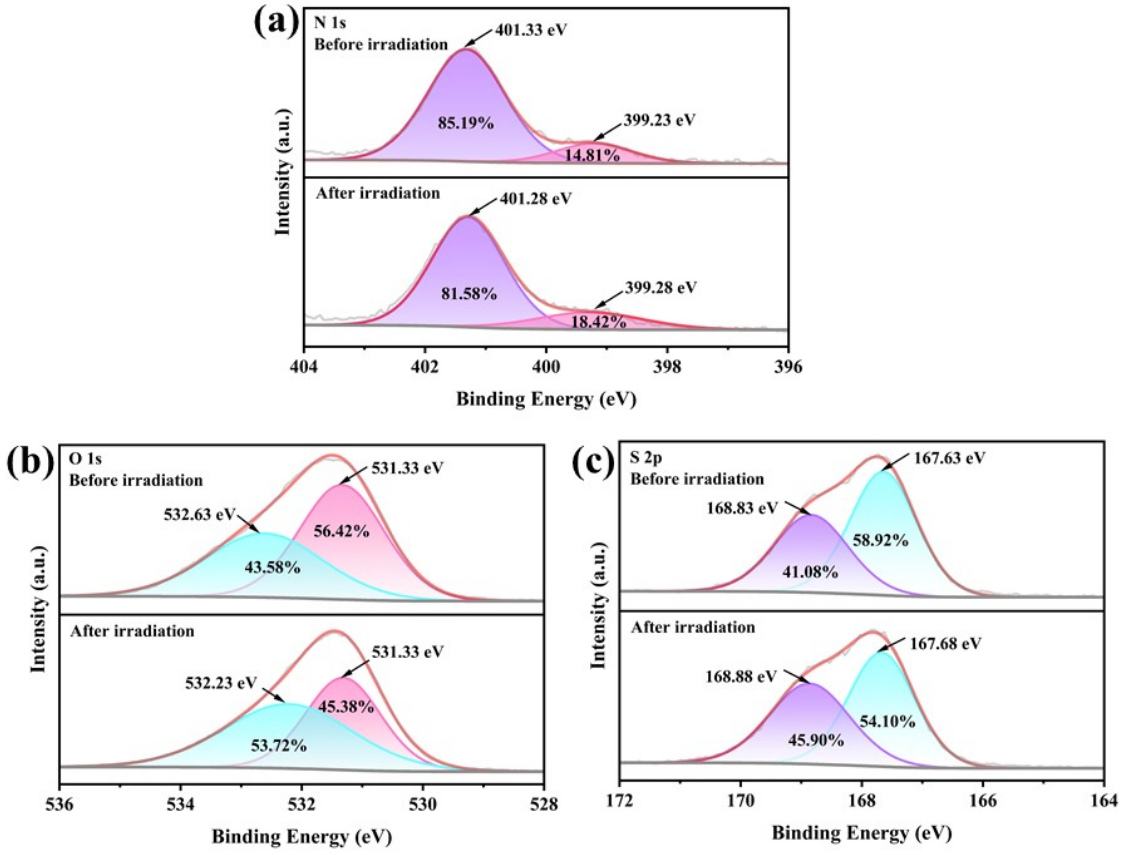

Figure S16. XPS spectra of **iHOF-71** before and after 365 nm UV irradiation: (a) N 1s, (b) O 1s, and (c) S 2p.

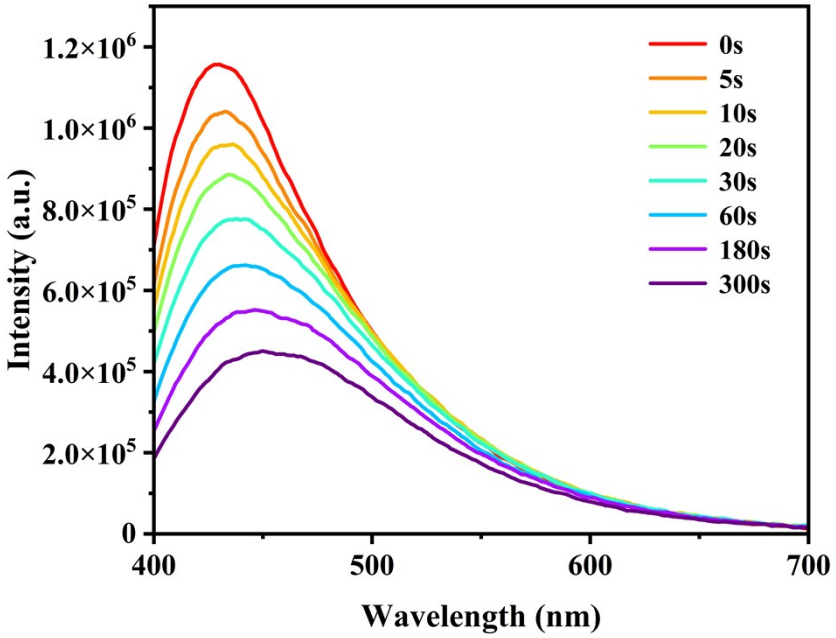

Figure S17. Fluorescence spectra of **iHOF-71** under UV irradiation (λex=365 nm).

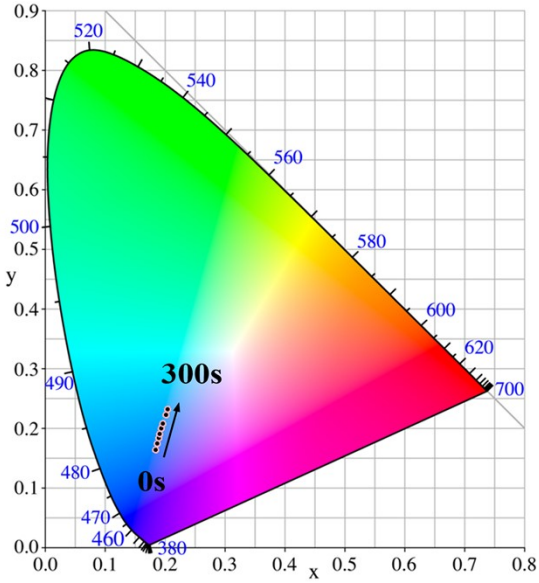

Figure S18. Corresponding CIE chromaticity diagram of the fluorescence decay curves for **iHOF-71**.

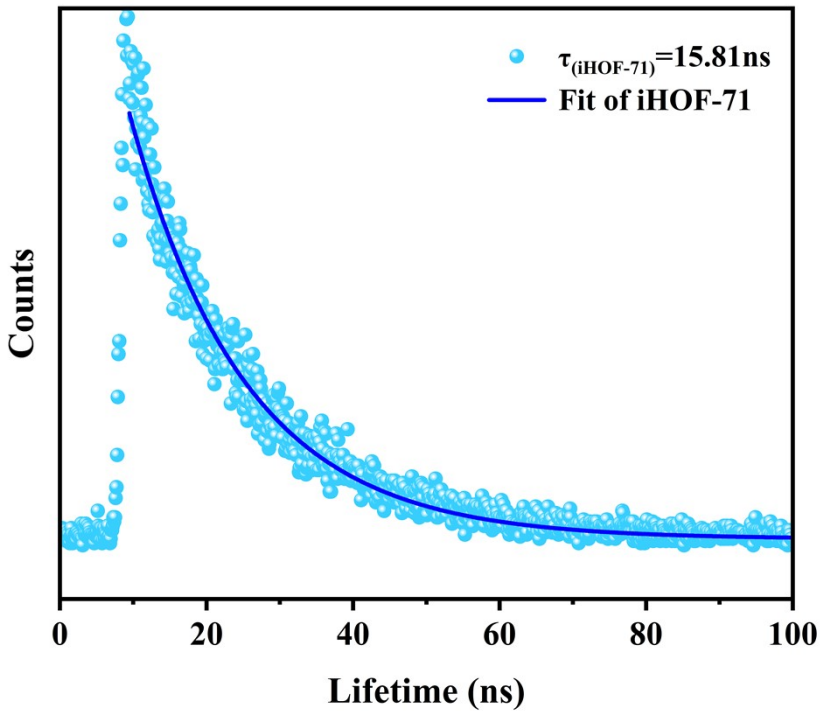

Figure S19. The fluorescence lifetime of **iHOF-71**.

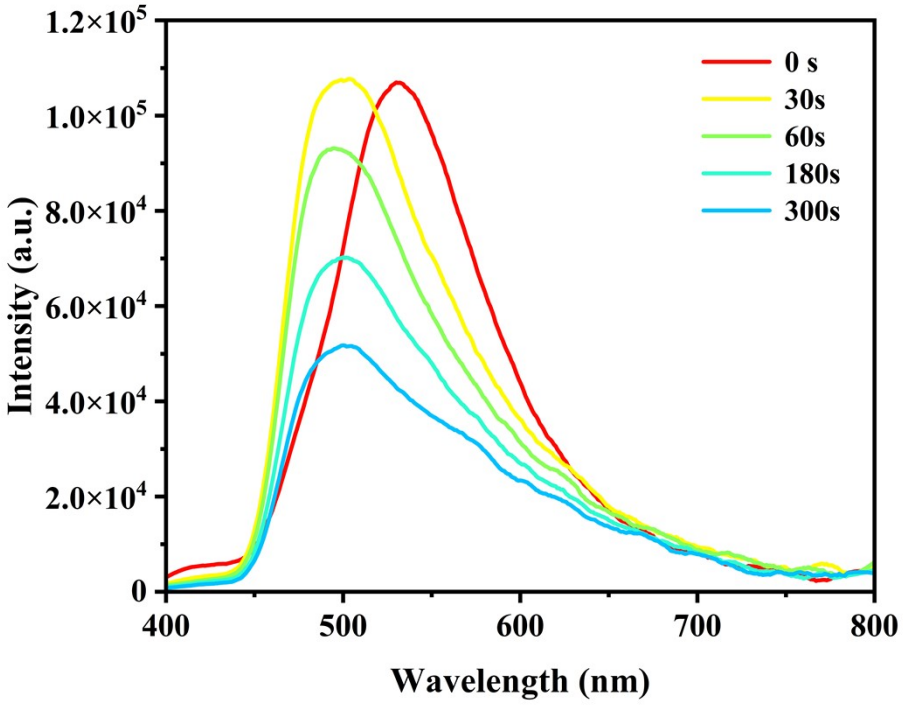

Figure S20. Time-dependent phosphorescence spectra of **iHOF-71** under UV irradiation (λ_{ex}=365 nm).

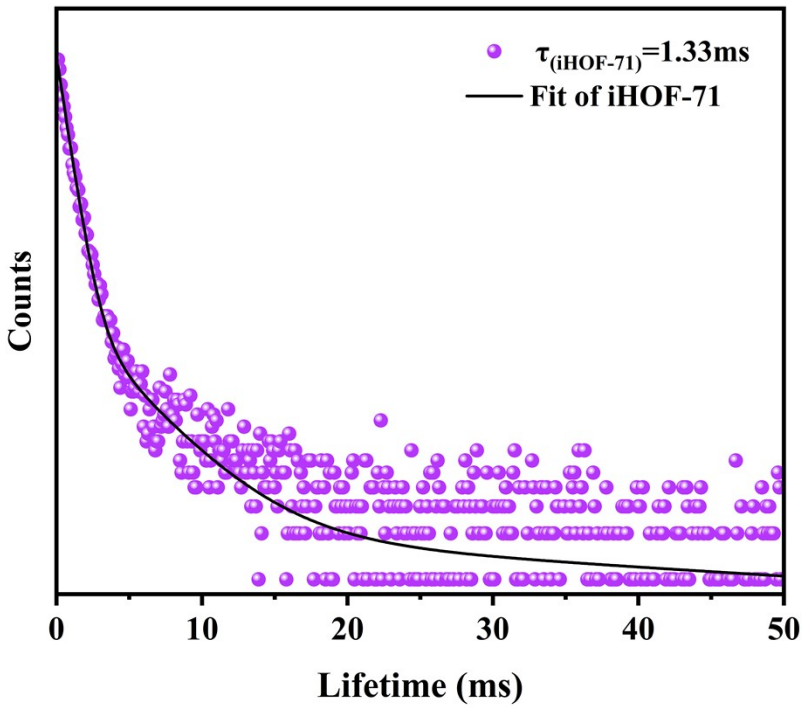

Figure S21. The phosphorescence lifetime of **iHOF-71**.

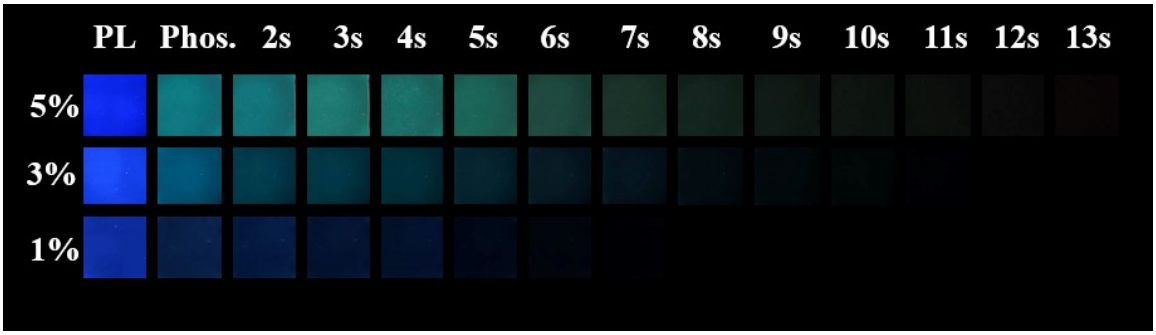

Figure S22. Fluorescence and phosphorescence decay images of the **1%**, **3%** and **5%-iHOF-71@PVA** composite membranes.

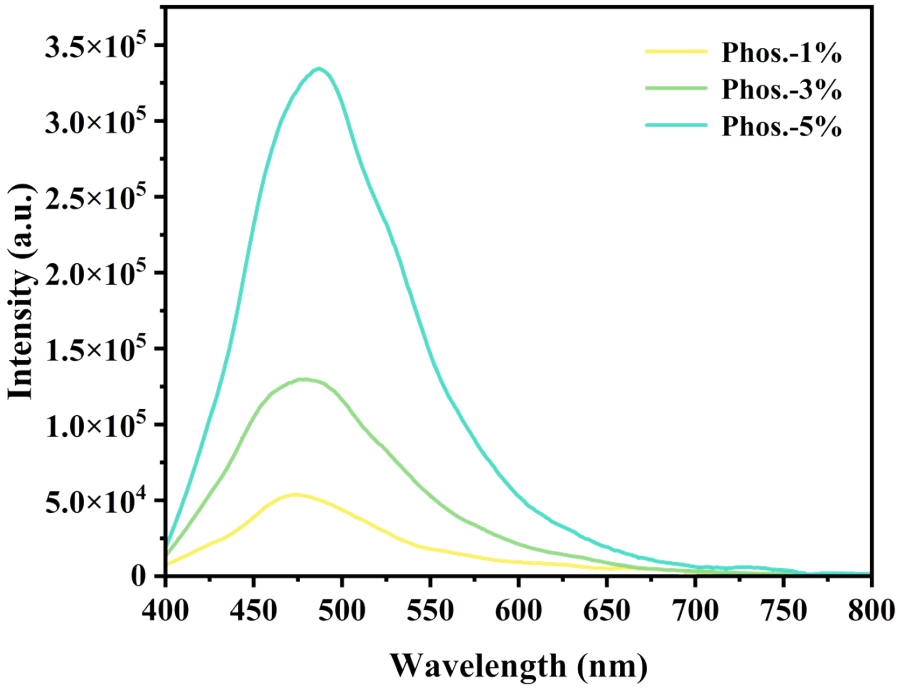

Figure S23. Phosphorescence spectra of **iHOF-71@PVA** composite membranes with different doping concentrations (1%, 3% and 5%) (λ_{ex}=365 nm).

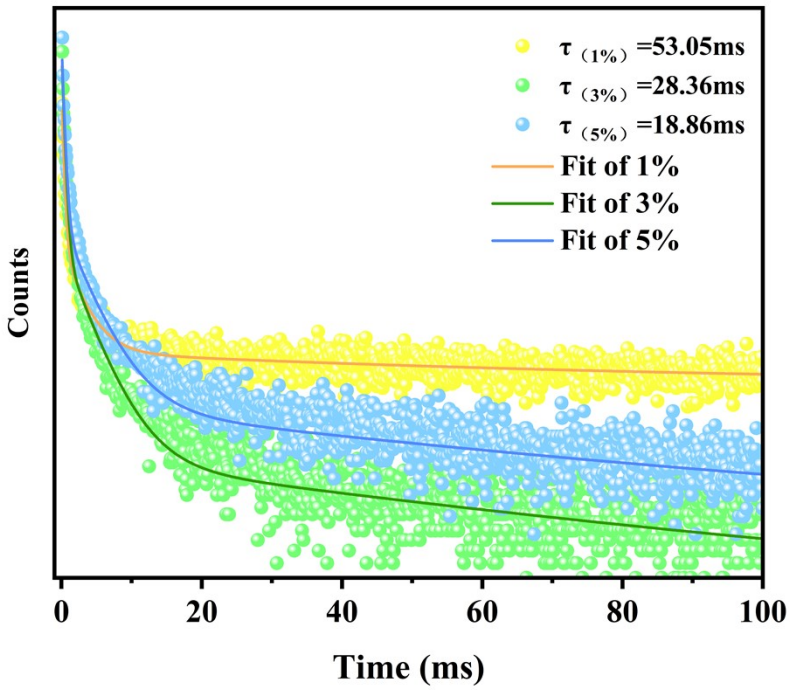

Figure S24. Phosphorescence lifetime of **iHOF-71@PVA** composite membranes with different doping concentrations (1%, 3% and 5%).

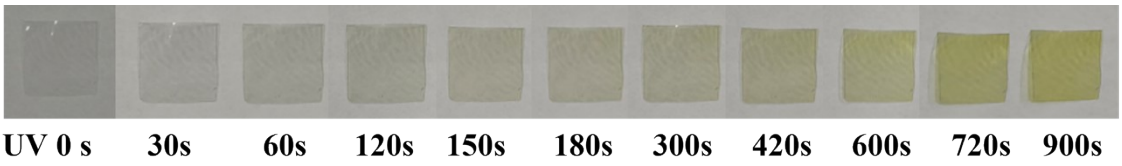

Figure S25. Photographs showing the color change of the **5%-iHOF-71@PVA** composite membrane under UV irradiation for different durations.

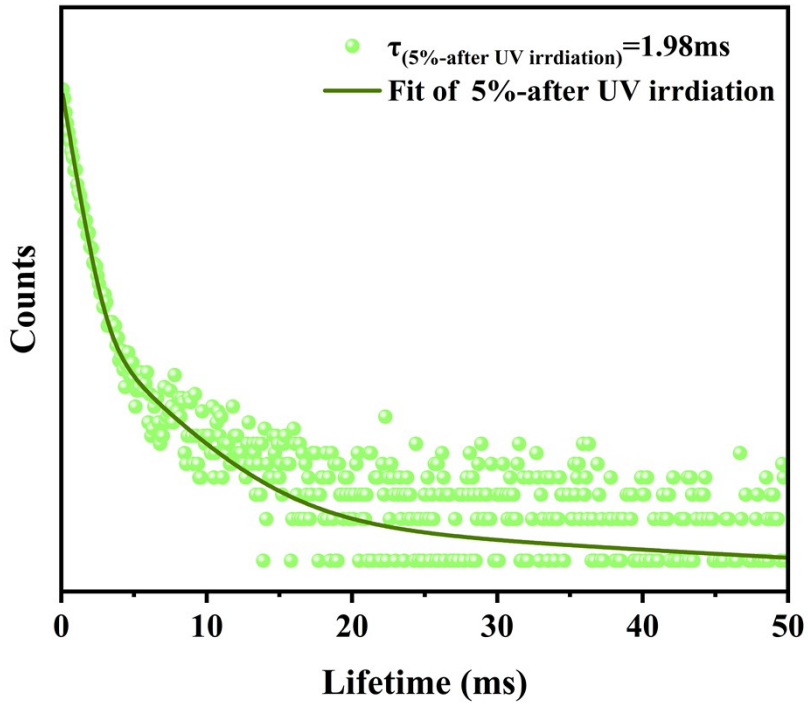

Figure S26. The phosphorescence lifetime of the **5%-iHOF-71@PVA** composite membrane after UV irradiation.

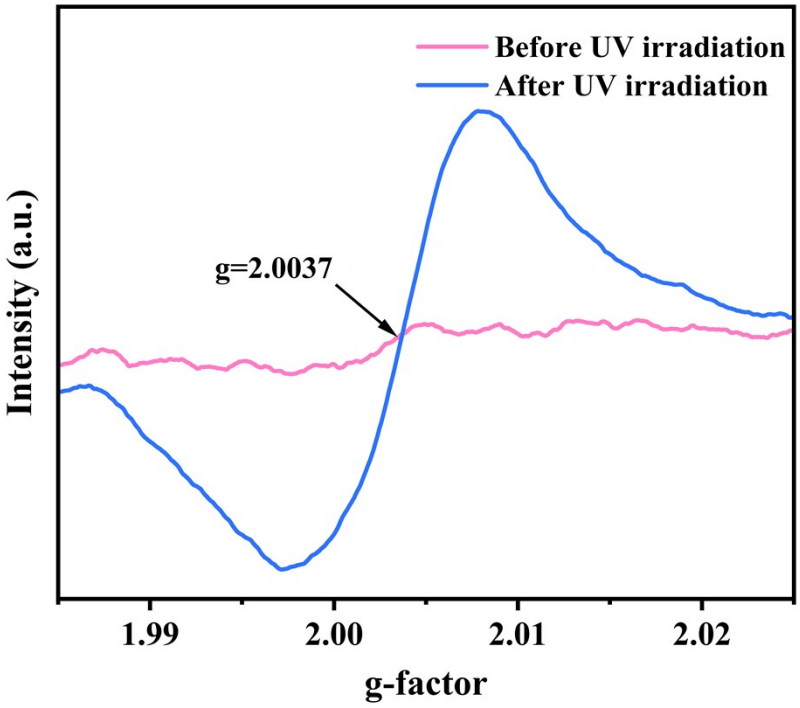

Figure 27. EPR spectra of the **5%-iHOF-71@PVA** composite membrane before and after UV (365 nm) irradiation.

Table S1. Crystal structure data and refinement details of **iHOF-71**.

iHOF-71	
Empirical formula	$C_{351}H_{456}N_{36}O_{174}S_{27}$
Formula weight	8829.11
Temperature / K	193.15(10)
Crystal system	trigonal
Space group	$P3_2$
a/Å	22.0448(9)
b/Å	22.0448(9)
c/Å	23.7361(13)
α/°	90
β/°	90
γ/°	120
Volume/Å^3	9989.7(10)
Z	1
ρ_{calc} g/cm^3	1.468
μ/mm^{-1}	0.251
F (000)	4638.0
Radiation	Mo Kα (λ = 0.71073)
2Θ range for data collection/°	3.696 to 55.096
Index ranges	-28 ≤ h ≤ 28, -28 ≤ k ≤ 28, -30 ≤ l ≤ 23
Reflections collected	93865
Independent reflections	27399 [R_{int} = 0.0984, R_{sigma} = 0.1021]
Data/restraints/parameters	27399/310/1870
Goodness-of-fit on F^2	1.085
Final R indexes [I>=2σ (I)]	R_1 = 0.1154, wR_2 = 0.2695
Final R indexes [all data]	R_1 = 0.1574, wR_2 = 0.2951
Largest diff. peak and hole / e. Å^{-3}	0.83/-0.58
CCDC number	2488490

[a] $R_1 = \sum||F_o|-|F_c||/\sum|F_o|$. [b] $wR_2 = \{\sum[w(F_o^2-F_c^2)^2]/\sum[w(F_o^2)^2]\}^{1/2}$

Table S2. Detailed data of **iHOF-71** hydrogen bonds.

		H Y / Å			
S1-O1	**H52A-O52**	**2.033 Å**	**S8-O22**	**H42A-O42**	**1.991**
S1-O2	**H30A-O30**	**1.974 Å**	**S8-O24**	**H38A-O38**	**2.058**
S1-O3	**H39B-O39**	**2.106**	**S9-O26**	**H45B-O45**	**2.128**
S1-O3	**H53B-O53**	**2.017**	**S9-O27**	**H39A-O39**	**1.885**
S2-O4	**H50B-O50**	**2.050**	**O40-H40A**	**O25-S9**	**1.895**
S2-O4	**H54B-O54**	**1.864**	**O42-H42B**	**O7-S3**	**2.057**
S2-O5	**H31A-O31**	**1.887**	**S4-O10**	**H43A-O43**	**1.937**
S2-O6	**H58B-O58**	**1.948**	**S4-O11**	**H28A-O28**	**1.908**
S3-O7	**H29B-O29**	**2.059**	**S4-O11**	**H32B-O32**	**2.0898**
S3-O7	**H42B-O42**	**2.057**	**S4-O12**	**H58A-O58**	**1.981**
S3-O8	**H30B-O30**	**2.164**	**S5-O13**	**H51B-O51**	**1.948**
S3-O8	**H36AO36**	**1.972**	**S5-O14**	**H37B-O37**	**1.966**
S3-O9	**H31B-O31**	**2.039**	**S5-O14**	**H46B-O46**	**1.866**
S6-O16	**H41A-O41**	**2.137**	**S5-O15**	**H35B-O35**	**2.075**
S6-O17	**H46A-O46**	**1.897**	**S7-O20**	**H55B-O55**	**2.000**
S6-O18	**H39A-O39**	**1.967**	**S8-O23**	**H48A-O48**	**2.043**
S6-O18	**H44A-O44**	**2.012**	**S9-O25**	**H29A-O29**	**2.035**
S7-O19	**H34B-O34**	**2.045**	**S9-O25**	**H40A-O40**	**1.895**
S7-O21	**H47A-O47**	**1.991**	**O30**	**H2-N2**	**1.752**
S7-O14	**H49B-O49**	**1.961**	**O40**	**H11-N11**	**1.786**

S8-O22	H40B-O40	1.930	O53	H3-N3	1.820
N4-H4	O31	1.794	O28-H28B	O29	1.843
N12-H12	O57	1.747	O32	H33A-O33	1.701
N10-H10	O49	1.811	O32-H32A	O34	1.788
O33	H7A-N7	1.760	O33-H33B	O52	2.204
O43	H6-N6	1.763	O35	H49A-O49	1.981
O46	H8A-N8	1.775	O35	H34A-O34	2.083
O28	H52B-O52	2.126	O35-H35A	O36	1.784
O37-H37A	O38	1.841	O36-H36B	O37	1.962
O38-H38B	O39	2.015	O43-H43B	O44	1.851
O41-H41B	O40	2.012	O44-H44B	O45	1.984
O47	H50A-O50	1.909	O45-H45A	O57	2.190
O47-H47B	O48	1.915	O45-H45A	O58	2.440
O48-H48B	O41	2.081	O55	H56A-O56	2.039
O50	H51A-O50	1.857	O55-H55A	O51	2.007
O53-H53A	O54	1.805	O56	H57B-O57	1.793
O54-H54A	O45	2.106	O57-H57A	O58	1.719

Supplementary Reference

(1) Y.-T. Li, M. Handke, Y.-S. Chen, A. G. Shtukenberg, C. H. T. Hu, and M. D. Ward. *J. Am. Chem. Soc.*, 2018, **140**, 12915-12921.

(2) M.-F. Huang, L.-H. Cao and B. Zhou, *Chem. Commun.*, 2024, **60**, 3437-3440.

(3) L. Krause, R. Herbst-Irmer, G. M. Sheldrick and D. Stalke, *J. Appl. Cryst.*, 2015, **48**, 3-10.

(4) L. J. Bourhis, O. V. Dolomanov, R. J. Gildea, J. A. K. Howard and H. Puschmann, *Acta Cryst. A*, 2015, **71**, 59-75.

(5) O. V. Dolomanov, L. J. Bourhis, R. J. Gildea, J. A. K. Howard and H. Puschmann, *J. Appl. Cryst.*, 2009, **42**, 339-341.